Journal of Materials Processing Tech. 262 (2018) 221–231

Contents lists available at ScienceDirect

Journal of Materials Processing Tech.

journal homepage: www.elsevier.com/locate/jmatprotec

Flow behaviors and microstructural evolutions of a novel high-Co powder metallurgy superalloy during hot working

Liming Tan[a,b,c], Guoai He[d,e], Yunping Li[a,b,c], Feng Liu[a,b,c,*], Yan Nie[f], Liang Jiang[a,b,c]

[a] State Key Laboratory of Powder Metallurgy, Central South University, Changsha 410083, China
[b] Powder Metallurgy Research Institute, Central South University, Changsha 410083, China
[c] High Temperature Materials Research Institute, Central South University, Changsha 410083, China
[d] State Key Laboratory of High Performance Complex Manufacturing, Central South University, Changsha 410083, China
[e] Light Alloy Research Institute, Central South University, Changsha 410083, China
[f] Yuanmeng Precision Technology (Shenzhen) Institute, Shenzhen, China

ARTICLE INFO

Keywords:
Nickel-based superalloy
High Co content
Flow behaviors
Hot working condition
Abnormally large grains

ABSTRACT

To understand how to tailor microstructure of high-Co polycrystalline superalloys during hot processing, the flow curves of a nickel-based superalloy with high Co content was quantitatively analyzed, and the microstructure evolution was studied by a high-throughput method. The results suggested that hot working conditions, especially the temperature, strongly influenced the grain structure at annealing. In specific, deforming under low strain rate and high temperature conditions facilitated the recovery and grain growth to consume the stored strain energy, furthermore, the weakened pinning effects of γ' precipitates accelerated these procedures, which made the high-Co superalloy more vulnerable to the formation of abnormally large grains during subsequent supersolvus annealing.

1. Introduction

As Pollock and Tin (2006) and Reed (2006) summarized, powder metallurgy nickel-based superalloys are widely used as turbine disks in advanced aircraft engines, due to their outstanding mechanical properties at the extreme environments. Recently, nickel-based superalloys with high fraction of Co have attracted much attention, since Co could improve the properties of nickel-based superalloys in several aspects: (1) lowering the γ' solvus temperature and widening heat treatment window, as Cui et al. (2009, 2008, 2006) and Gu et al. (2009) said; (2) reducing the lattice misfit and interface energy between γ' phase and γ matrix, which is benefit to refine and stabilize the γ' precipitates, as Bian et al. (2015) found; (3) promoting the planar slip during deformation and enhances creep resistance, which was concluded by Gu et al. (2009) and Jones et al. (2014); (4) improving the hot workability through accelerating the process of dislocation accumulation and dynamic recrystallization (DRX) during hot deformation, as Li et al. (2017b) explored. Although numerous results have proved the above-mentioned points of (1) - (3), the mechanisms of grain structure evolution during hot deformation and heat treatment of high Co nickel-based polycrystalline superalloys have not been clarified clearly.

In specific, increased Co addition has an impact on microstructure evolution during hot deformation and subsequent annealing, which is closely related with the low SFE, as Li et al. (2017b) stated. The reduced SFE facilitates the perfect dislocation dissociate into partial dislocations with wider stacking faults and makes dislocation recovery more difficult, dislocation accumulation and discontinuous dynamic recrystallization (DDRX) are then enhanced during deformation at elevated temperatures, as reported by Buckingham et al. (2016); Chen et al. (2014), (Huang and Logé, 2016), and Tan et al. (2017). However, few works concern how the microstructure of this kind superalloy changes at different hot working conditions, which is essential to the optimization of processing parameters.

Pérez (2018) and Park et al. (2001) concluded that the hot working variables, including temperature, strain, strain rate, and thereafter annealing play critical roles in tailoring microstructure of the polycrystalline superalloys. By compressing double cone (DC) specimens to generate gradient distribution of strain in a single sample, the effects of these processing parameters could be efficiently studied, as introduced by Semiatin et al. (2004) and He et al. (2017a). Since this high throughput method was applied in this work, finite element method was indispensable to identify the changes of stress, strain and strain rate in different regions of DCs. In this study, more emphasis was put on the interactions among grain boundary, dislocation, and γ' particle during different hot working conditions; and the formation of abnormally large grains (ALGs) after supersolvus annealing was studied regarding the

---

[*] Corresponding author at: State key laboratory of powder metallurgy, Central South University, #932 south Lushan road, Yuelu district, Changsha, Hunan province, 410083, PR China.
E-mail address: liufeng@csu.edu.cn (F. Liu).

https://doi.org/10.1016/j.jmatprotec.2018.06.039
Received 8 April 2018; Received in revised form 26 May 2018; Accepted 25 June 2018

Table 1
Nominal composition of A1 in wt.%.

Ni	Co	Cr	Al	Ti	W	Mo	Nb	Hf	C	B	Zr
Bal.	26.0	13.0	3.2	3.7	4.0	4.0	0.95	0.2	0.05	0.009	0.05

stored strain energy.

2. Materials and methods

The adopted material A1 is a newly developed high Co nickel-based superalloy, which is strengthen by γ' precipitates with solvus temperature around 1154 °C, as indicated by Wu et al. (2017) and He et al. (2017c). The nominal composition of A1 is listed in Table 1. Fractions of equilibrium precipitates at high temperatures of A1 was calculated by using the Thermo-Calc program with TTNi8 database.

The cylinder and DC specimens were prepared by powder metallurgy (P/M) route, specifically, through vacuum inducing melting (VIM), plasma rotating electrode process (PREP) atomization to produce 50 ~ 100 μm powders, hot isostatic pressing (HIP) at 1100 °C and 140 MPa, and hot extrusion (HEX) at 1100 °C with area reduction ratio of 10:1, as described in previous research conducted by He et al. (2017b) and Tan et al. (2017). The average grain size of extruded alloys was detected to be around 13.4 μm (ASTM 9.5), and the cylinder specimen was 8 mm in diameter and 12 mm in height.

To obtain the true stress-strain curves of cylinder specimens, the hot compression tests were performed on the Gleeble 3180D thermal simulator (Dynamic Systems, Inc., New York, New York). The specimens are compressed to a final true strain of 0.7 under temperatures ranging from 1000 °C to 1100 °C and strain rates from 0.001 to 1.0 s^{-1}. In terms of the isothermal forging on DC specimens, the geometry of DC and practical procedures are shown in Fig. 1. Specifically, DCs were heated to certain temperatures and hold for 15 min., followed by isothermal compression on MTS machine (810.13) at different conditions, thereafter they were immediately quenched in water to frozen the instant microstructure. After that, the specimens were annealed at supersolvus temperature 1165 °C for 1 h to exam their sensitivity to ALG formation.

The constitutive equation describing plastic behavior adopted by Deform were deduced from true stress-strain data by compressing cylinder specimens. Finite element method (FEM) software Deform simulation package (SFTC, Ohio/USA) 3D V6.1 was applied to simulate the distribution of strain and stress during deformation.

In order to observe microstructure evolution in DC by EBSD, the specimens cut parallel to the compression direction was polished by abrasive papers and 50 nm colloidal silica, followed by vibration polishing for 8 h. Electron back-scattered diffraction (EBSD) and scanning electron microscope (SEM) observations were performed by field-emission SEM (FEI Quanta 650) equipped with an EBSD detector. The EBSD data were analyzed via HKL Channel 5 software, and the grain size was described by equivalent diameter $2\sqrt{\frac{S_{\mathrm{Grain}}}{\pi}}$, where S_{Grain} was the area of each grain. Local misorientation component in Channel 5 was adopted to characterize the hardening state of individual grains as introduced by Detrois et al. (2016), which is similar with the Grain Orientation Spread (GOS) (Agnoli et al., 2015; Bober et al., 2017) in TSL OIM Analysis software. Optical microscope (LEICA-DM4000 M, Leica Microsystems, Wetzlar, Germany) was used to determine the overall distribution of the abnormally large grains in annealed DCs.

To observe γ' phase by SEM, the polished samples were etched in a reagent (33 vol.% HNO_3, 33 vol.% acetic acid, 33 vol.% H_2O, 1 vol.% HF) for 30 to 60 s. Transmission electron microscope (TEM) observation was performed on field-emission TEM Tecnai G2 F20, FEI with 200 kV accelerating voltage, to inspect the interactions among grain or subgrain boundary, dislocation, and γ' particle. To prepare TEM samples, slices in diameter of 3 mm were cut from medium positions in DCs with thickness of about 50 μm, and twin-jet electropolished then in a corrosive reagent (90 vol.% ethanol plus 10 vol.% perchloric acid) at −25 °C and 20 V. Fig. 2 presents the methods of preparing EBSD and TEM specimens.

3. Results and discussion

3.1. Quantitative analysis on flow behavior

The true stress-strain curves of cylinder specimens hot-compressed at different conditions are illustrated in Fig. 3. The results suggest that the flow stress reduces with decreasing strain rates and increasing temperatures during hot compression, which is unanimous with other nickel-base superalloys, such as Alloy 617B (Jiang et al., 2015), Haynes230 (Liu et al., 2008), FGH4096 (Ning et al., 2010), and Inconel 718 (Yuan and Liu, 2005). Based on the true stress and strain curves, it can be justified that specimens orderly experience periods of work hardening caused by dislocation accumulation, softening because of recovery and recrystallization, and steady state when strains get higher.

In this work, the hyperbolic-sine Arrhenius-type equation is chosen to express constitutive relationships, as initially proposed by Sellars and Tegart, which has already been applied by Bi et al. (2010), and He et al. (2015):

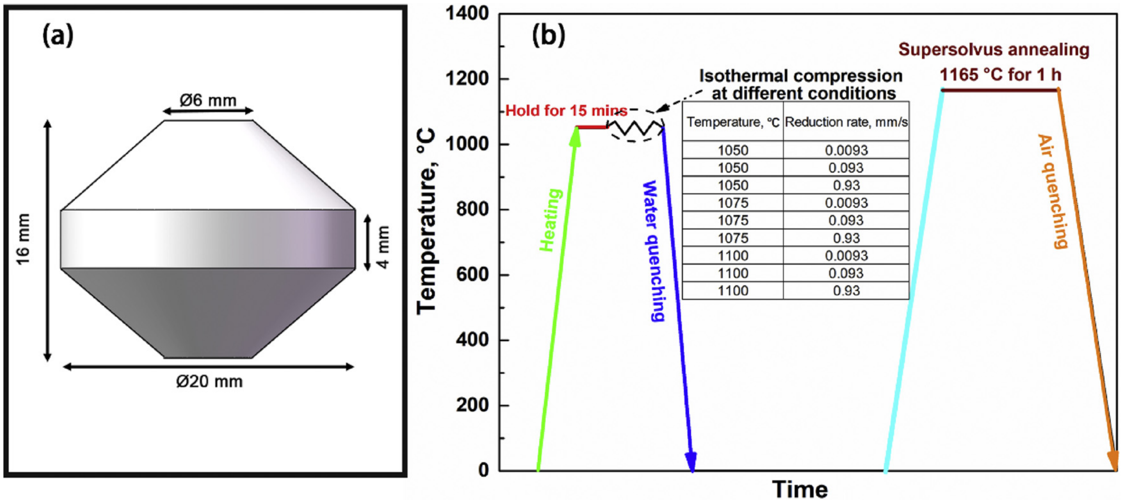

Temperature, °C	Reduction rate, mm/s
1050	0.0093
1050	0.093
1050	0.93
1075	0.0093
1075	0.093
1075	0.93
1100	0.0093
1100	0.093
1100	0.93

Fig. 1. The geometry and processing procedure of double cone specimens, wherein: (a) the geometry of double cone specimen; and (b) diagram showing isothermal compression and thereafter annealing conditions.